Effect of growth temperature on defect states of GaNAsSb intrinsic layer in GaAs/GaNAsSb/GaAs photodiode for 1.3μm application

Satrio Wicaksono, Soon Fatt Yoon, Wan Khai Loke, Kianhuan Tan, Kim Luong Lew, Malek Zegaoui, Jean-Pierre Vilcot, Didier Decoster, Jean Chazelas

▶ **To cite this version:**

Satrio Wicaksono, Soon Fatt Yoon, Wan Khai Loke, Kianhuan Tan, Kim Luong Lew, et al.. Effect of growth temperature on defect states of GaNAsSb intrinsic layer in GaAs/GaNAsSb/GaAs photodiode for 1.3μm application. Journal of Applied Physics, 2007, 102 (4), pp.044505. 10.1063/1.2769801 . hal-00283082

HAL Id: hal-00283082
https://hal.science/hal-00283082

Submitted on 25 May 2022

HAL is a multi-disciplinary open access archive for the deposit and dissemination of scientific research documents, whether they are published or not. The documents may come from teaching and research institutions in France or abroad, or from public or private research centers.

L'archive ouverte pluridisciplinaire **HAL**, est destinée au dépôt et à la diffusion de documents scientifiques de niveau recherche, publiés ou non, émanant des établissements d'enseignement et de recherche français ou étrangers, des laboratoires publics ou privés.

Journal of Applied Physics

Effect of growth temperature on defect states of GaAsSbN intrinsic layer in GaAs / GaAsSbN / GaAs photodiode for 1.3 μm application

Cite as: J. Appl. Phys. **102**, 044505 (2007); https://doi.org/10.1063/1.2769801
Submitted: 12 February 2007 • Accepted: 02 July 2007 • Published Online: 23 August 2007

S. Wicaksono, S. F. Yoon, W. K. Loke, et al.

View Online Export Citation

ARTICLES YOU MAY BE INTERESTED IN

Defect-induced trap-assisted tunneling current in GaInNAs grown on GaAs substrate
Journal of Applied Physics **102**, 054501 (2007); https://doi.org/10.1063/1.2775908

Improvement of GaInNAs *p-i-n* photodetector responsivity by antimony incorporation
Journal of Applied Physics **101**, 033122 (2007); https://doi.org/10.1063/1.2435990

N-polar GaN / AlGaN / GaN high electron mobility transistors
Journal of Applied Physics **102**, 044501 (2007); https://doi.org/10.1063/1.2769950

Lock-in Amplifiers up to 600 MHz
Zurich Instruments
Watch

AIP Publishing

© 2007 American Institute of Physics.

Effect of growth temperature on defect states of GaAsSbN intrinsic layer in GaAs/GaAsSbN/GaAs photodiode for 1.3 μm application

S. Wicaksono,[a] S. F. Yoon, W. K. Loke, K. H. Tan, and K. L. Lew
School of Electrical and Electronic Engineering, Nanyang Technological University, Nanyang Avenue, Singapore 639798, Republic of Singapore

M. Zegaoui, J. P. Vilcot, and D. Decoster
Institute of Electronics, Microelectronics and Nanotechnology (IEMN), UMR CNRS 8520, Université des Sciences et Technologies de Lille, BP 60069, 59652 Villeneuve d'Ascq Cedex, France

J. Chazelas
Thales Airborne Systems, 2 Avenue Gay Lussac, 78852, Elancourt, France

(Received 12 February 2007; accepted 2 July 2007; published online 23 August 2007)

A GaAsSbN layer closely lattice matched to GaAs was used as an intrinsic layer (*i* layer) in a GaAs/GaAsSbN/GaAs *p-i-n* photodiode with response up to 1.3 μm. Deep level transient spectroscopy measurement on the GaAs/GaAsSbN/GaAs reveals two types of hole traps (HTs) in the GaAsSbN *i* layer; (i) HT_1: a shallow N-related defect state ($E_a \sim 0.10-0.12$ eV) and (ii) HT_2: an As_{Ga} point defect-related midgap defect state with $E_a \sim 0.42-0.43$ eV. Reduction in growth temperature from 480 to 420 °C reduces the HT_2 trap concentration from 4×10^{15} to 1×10^{15} cm^{-3}, while increases the HT_1 trap concentration from 1×10^{14} to 7×10^{14} cm^{-3}. Reduction in the HT_2 trap concentration following growth temperature reduction was attributed to the suppression of As_{Ga} point defect formation. Evidence of possible change of the As_{Ga} midgap state to a shallow level defect due to the formation of $(As_{Ga}-N_{As})$ pairs was also suggested to have increased the HT_1 trap concentration and reduced the HT_2 trap concentration. An ~4 dBm improvement in photoresponse under 1.3 μm laser excitation and approximately eight times reduction in dark current at −8 V reverse bias were attributed to the reduction in the overall trap concentration and mainly the reduction of the As_{Ga}-related midgap trap concentration in the sample grown at 420 °C. © *2007 American Institute of Physics*. [DOI: 10.1063/1.2769801]

I. INTRODUCTION

GaAsSbN has been proposed as a potential material for GaAs-based optoelectronic devices.[1] The material has been extensively studied as a barrier layer for GaAs-based vertical cavity surface emitting laser (VCSEL) using GaInNAsSb/GaAsSbN multiquantum well (MQW) as the lasing material.[2,3] Others reported the use of $GaAs_{0.615}Sb_{0.36}N_{0.025}$/GaAs strained double quantum well structure in a *p-i-n* photodiode with responsivity of 0.01 A/W at 1.55 μm wavelength.[4] Another approach in using GaAsSbN is to tune the concentrations of N and Sb to allow close lattice matching to GaAs while reaching the band gap energy for the desired applications. The close lattice-matched condition to GaAs allows the application of ~0.45 μm thick GaAsSbN as the *i* layer of the photodiode.[5] Recently, GaAs/GaAsSbN/GaAs photodiodes grown by molecular beam epitaxy (MBE) have been reported with responsivity up to 0.033 A/W at 1.3 μm wavelength. X-ray diffraction (XRD) reciprocal space mapping study on GaAs/GaAsSbN/GaAs photodiodes suggests that lower growth temperature suppresses the formation of point defects during the growth of the GaAsSbN *i* layer.[6]

Recent x-ray absorption fine-structure (XAFS) experiment on the Sb *K*-edge x-ray absorption of GaAsSbN/GaAs samples has shown evidence of Sb–Sb short range order clustering.[7] However, further experiments on the other constituent atoms have not been reported. Furthermore, first-principles calculation simulation results on the formation energy of the native defects in GaAsSbN and the effect of those defects on the band structure are currently not available for reference. Thus, it has to be assumed that some of the native defects present in GaAs, GaNAs, and GaInNAs can be found in GaAsSbN given the similar growth conditions. For instance, the formation of N–N split interstitials, N–As split interstitials, nearest neighbors $(As_{Ga}-N_{As})$, and $(V_{Ga}-N_{As})$ pairs as native defects in GaNAs have been predicted by first-principles calculation.[8] Another first-principles calculation result on GaNAs also suggests shallow acceptor level related to Ga vacancies (V_{Ga}) at 0.03–0.18 eV above the valence band maximum (VBM).[9] N–As and N–N split interstitials in GaNAs have been detected indirectly by combination of secondary ions mass spectroscopy (SIMS) and high resolution x-ray diffraction (HR-XRD) of GaNAs due to the GaNAs lattice constant deviation from Vegard's law.[10,11] Positron-annihilation measurement and nuclear reaction analysis (NRA) on Rutherford backscattering spectroscopy (RBS) experiments have shown traces of N interstitials and gallium vacancies in GaNAs and GaInNAs.[12–14] Optically detected magnetic resonance (ODMR) measurement also found evidence of As_{Ga} in GaNAs.[15,16] The presence of the As_{Ga} and V_{Ga} is expected due to the similarities of growth

[a]Electronic mail: satrio@ntu.edu.sg

 © 2007 American Institute of Physics

conditions of the dilute nitride materials with the low temperature (LT) GaAs.[17] The GaAsSbN *i* layer was also grown at low temperature (<500 °C) under As-rich condition to prevent Ga–N phase separation and promote two-dimensional (2D) layer-by-layer growth.[18] In fact, LT GaAs grown at 400 °C have been reported with high concentration of the EL2 midgap defects ($\sim 10^{19}$ cm^{-3}).[19] The presence of this midgap defect is expected in GaInNAs and GaAsSbN, as similar EL2 defects have been observed recently in GaNAs.[20]

Recently, DLTS was also used to study the presence of defects in closely lattice-matched GaInNAs absorption layer with the band gap of 1 eV for multijunction solar cells,[21–26] base material in *n-p-n* GaAs-based heterojunction bipolar transistor (HBT),[27] and *i* layer in GaAs-based photodiode.[28] The presence of a midgap trap along with some N-related shallow traps has been found to exhibit nonlocalized defect behavior that indicate continuous distribution of states or discrete but closely spaced energy levels.[29–31] Although several authors suggest that the midgap defect state may have resembled the EL2 defect,[26,27] theoretical or experimental studies on GaAsSbN are still lacking. Therefore, DLTS measurement results on GaAs/GaAsSbN/GaAs *p-i-n* structures with the GaAsSbN *i* layers grown at 480 and 420 °C will be presented in this work. The measurement reveals two types of hole traps (HTs) in the GaAsSbN *i* layer. The improvement in the photodiode performance and XRD reciprocal space mapping results is consistent with the correlation found between the *i* layer growth temperature and the trap concentrations. These results have provided useful insight for the future applications of GaAsSbN.

II. EXPERIMENTAL PROCEDURE

GaAs/GaAsSbN/GaAs photodiodes were grown on *n*+ GaAs substrates using solid source molecular beam epitaxy (SSMBE) with arsenic (As) and antimony (Sb) valved cracker sources in conjunction with a radio frequency (rf) plasma nitrogen source. The MBE chamber is equipped with carbon tetrabromide (CBr_4) gas source and standard Si effusion cell as *p*-type and *n*-type dopant sources, which are calibrated to deliver doping concentrations of $\sim 1 \times 10^{19}$ (*p* type) and $\sim 5 \times 10^{18}$ cm^{-3} (*n* type), respectively. Two samples of GaAs/GaAsSbN/GaAs photodiodes were grown with *i* layer thickness of ~0.45 μm under different growth temperatures of the *i* layer. The growth temperature of the *p*-type and *n*-type GaAs layers was kept constant at 580 °C, while the *i*-layer growth temperatures were kept at 480 °C for sample A and 420 °C for sample B. The Sb flux was tuned to achieve a close lattice-matched condition of GaAsSbN to GaAs, while the N source rf power of 500 W and 0.1 SCCM (SCCM denotes standard cubic centimeter per minute at STP) N_2 gas flow were kept the same between the two samples. During the growth of the *i* layer, the growth rate was lowered from 1 to 0.2 μm/h to increase the N incorporation to ~2%, which is essential to achieve 1.3 μm wavelength response. The Sb and N concentrations were measured by SIMS with Cs^+ as the primary ion source. The Sb concentration was found to be 6% (±0.3%) for both samples A and B. The nitrogen concentrations are 2.5% (±0.2%) for sample A and 2.8% (±0.2%) for sample B.[6]

Standard fabrication procedure was carried out on the back-polished *p-i-n* samples. Ohmic contacts were made by depositing Ti/Au and Ge/Ni/Au alloys on the *n* and *p* sides of the sample, respectively. To minimize surface leakage current, photodiode mesa structures were fabricated. Mesa structures with 200 μm ring diameter were formed using standard lithography process without surface passivation. High frequency photoresponse measurement was carried out on the photodiodes by exciting the devices with a 1.3 μm laser coupled to a single mode optical fiber with calibrated power of 5 mW. The laser was modulated using a rf sweep generator from 10 MHz to 26.5 GHz. The frequency response from the photodiode was measured by a spectrum analyzer.

For deep level defects study purposes, capacitance-voltage (*C-V*) and DLTS measurements were carried out on samples A and B using a digital DLTS system equipped with a 1 MHz bridge capacitance meter. Deep level transient Fourier spectroscopy (DLTFS) was conducted by sampling *N* values from each capacitance transients measured at different temperatures from 40 to 340 K. Discrete Fourier coefficients were obtained from these transient measurements, from which the time constant of the carrier emission can be calculated as follows:[32]

$$\tau = \frac{1}{n\omega}\frac{b_n}{a_n}, \tag{1}$$

where τ is the carrier emission time constant, a_n and b_n, are the cosine and sine coefficients of the *n*th order, *n* is the order of the coefficients, and $\omega = 2\pi/T_W$, where T_W is the period width.

Fourier transform can be carried out on the recorded capacitance transients $C(t)$ using

$$C(t) = f(t) = \frac{a_0}{2} + \sum_{n=1}^{N-1} a_n \cos(2\pi nt/T_W) + \sum_{n=1}^{N-1} b_n \sin(2\pi nt/T_W), \tag{2}$$

where $n = 0, 1, 2, \ldots, N$, a_0 is the transient offset, t is the time, and N is the amount of sampling on the transient ($N = 512$ in this work). To obtain the activation energy E_a and the carrier capture cross section (σ_∞), a plot of $\ln(\tau T^2)$ vs $1000/T$ must be obtained. Thus, E_a and σ_∞ can be obtained from the standard Arrhenius equation for carrier emission,[33]

$$\ln(\tau T^2) = \frac{E_a}{kT} - \ln(\sigma_\infty \gamma_n), \tag{3}$$

where σ_∞ is the carrier capture cross section, $\gamma_n = 3.256 m_p^* \times 10^{21}$ cm^{-2} s^{-1} K^{-2}, and m_p^* is the hole effective mass ratio. In addition, the activation energy obtained from the Arrhenius analysis is often referred to as the apparent activation energy, which is the sum of the true activation energy and the cross-section activation energy.[30] This cross-section activation energy ΔE_σ can be correlated to the carrier capture cross section by

$$\sigma(T) = \sigma_\infty \exp(-\Delta E_\sigma / k_B T), \quad (4)$$

where k_B is the Boltzmann constant and T is the temperature where the DLTS signal maxima occurs. Thus by obtaining the hole capture cross section $\sigma(T)$, the true activation energy and ΔE_σ of the defect states can be determined.

The strained quantum well studies on GaAsSb suggest that the materials are miscible at least for Sb concentration up to 33%.[34] Delvin *et al.* have used $m_p^*=0.51-0.11x$ for $GaAs_{1-x}Sb_x$, which gives $m_p^*=0.50$ for Sb concentration $<\sim 10\%$.[35] The use of the band anticrossing (BAC) model[36] suggests that for GaAsSbN, only the valence band is only affected by Sb.[37–39] However, the low N concentration miscibility gap causes some complications in the theoretical prediction of dilute nitride materials[40] that render the simple interpolation method inaccurate.[41] Recently, calculation of the valence band structure of GaAsSbN/GaAs strained quantum wells using the multiband effective mass theory in conjunction with the BAC model has shown that increase of Sb concentration decreases the average hole effective mass ($\bar{m}_p^*$) value and increase of N concentration increases the $\bar{m}_p^*$.[42] The calculation yielded $\bar{m}_p^*=0.54$ for GaAsSbN with 2.5% N and 8% Sb, which is close to our N and Sb concentrations. On the other hand, the assumptions used in the BAC model have limited its ability to predict the perturbations of the valence band caused by N atoms,[43] particularly when N-related interstitial defects are involved.[44] However, assuming the concentration of N-interstitial defects is negligible compared to the substitutional ones, the assumption of the BAC model still holds. Therefore, in this work, $m_p^*=0.50$ will be used for the DLTS calculations.

III. RESULTS AND DISCUSSION

A. Capacitance-voltage, dark current, and photoresponsivity characteristics

Room temperature capacitance-voltage (C-V) measurements on the photodiode samples were used to determine the net acceptor concentration of the i layer (Fig. 1). As shown in the inset, the plot of $1/C^2$ vs V formed a straight line for both photodiodes. This suggests uniform background doping concentration profile of the i layer for both photodiodes. The p-type doping concentrations were found to be 1.1×10^{17} and 2.7×10^{17} cm^{-3} for i layers grown at 480 °C (sample A) and 420 °C (sample B), respectively.

The current-voltage (I-V) plots of samples A and B under nonilluminated conditions are shown in Fig. 2. Another photodiode sample with GaAsSbN i layer grown at 520 °C is included for comparison (sample C). The increase in leakage current with reverse bias voltage in sample A is faster than in sample B, with current density difference of approximately eight times at 8 V reverse bias (1.0 mA/cm^2 for sample B and 8.5 mA/cm^2 for sample A). As the surface leakage is minimized by the mesa structures, the quality of the i layer is reflected by the dark current behavior. This can be seen clearly in the extremely high leakage current in sample C ($\sim$17 A/cm^2 at −8 V). It suggests that the i layer in sample C is highly defective due to the high growth temperature which is unfavorable for 2D layer-by-layer dilute nitride growth.[18]

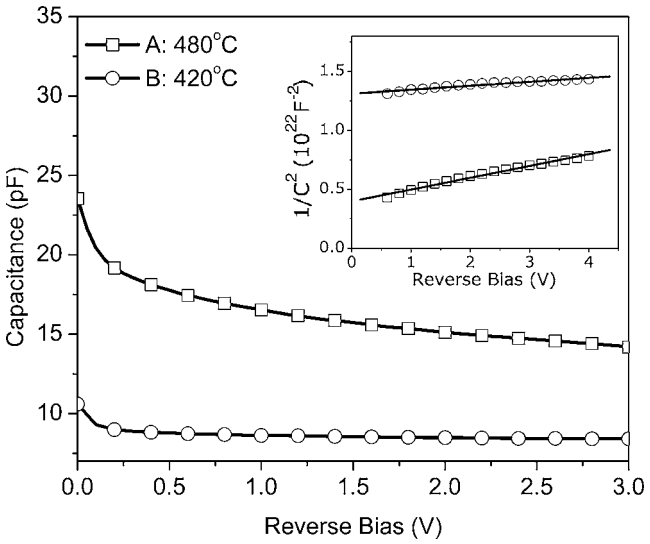

FIG. 1. Room temperature C-V plot of photodiodes with i layer grown at 480 and 420 °C. Inset: Plot of $1/C^2$ vs V from which the background doping concentration was determined.

Figure 3 shows the dynamic photoresponse results under 1.3 μm laser excitation, where the photodiodes exhibit 3 dBm cutoff frequencies ($f_{3\ dB}$) of 200, 260, and 130 MHz for samples A, B, and C, respectively. As the surface leakage current is minimized by the mesa structure, the $f_{3\ dB}$ will be greatly influenced by the quality of the i layer. The direct current (dc) photoresponse spectra of samples A, B, and C measured under 1 V reverse bias are shown in the inset. It is obvious that higher responsivity is obtained at 1.0 μm wavelength and that low temperature grown samples (A and B) show higher responsivity value. This is confirmed by the dynamic responsivity measurements at 1.3 μm laser excitation (Fig. 3), where sample B exhibits the best photoresponse (−38 dBm at the low frequency plateau region) as compared to sample A (−42 dBm) and sample C (−52 dBm). However,

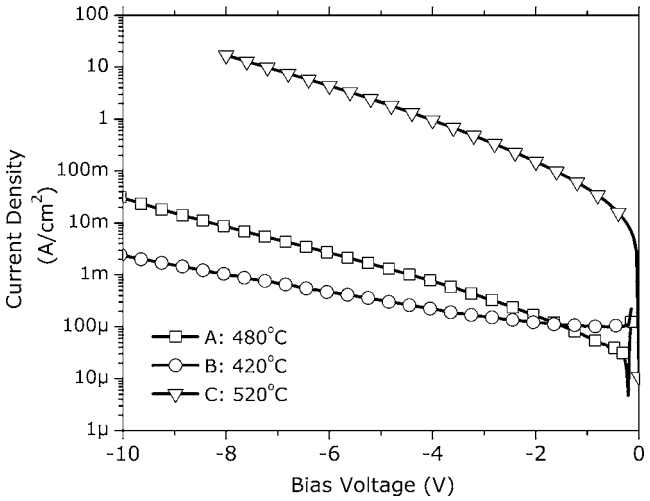

FIG. 2. Dark current characteristics of GaAs/GaAsSbN/GaAs photodiode (200 μm mesa diameter) with GaAsSbN i layers grown at different temperatures. Sample C with i layer grown at 520 C is added for comparison.

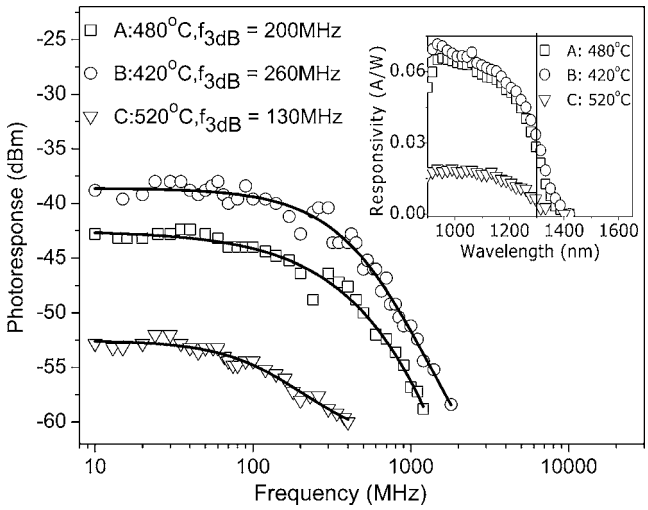

FIG. 3. Photoresponse of GaAs/GaAsSbN/GaAs photodiodes with GaAsSbN *i* layer grown at different temperatures measured with 1.3 μm laser excitation under −1 V reverse bias. (The line serves as a guide for the eyes.) Inset: dc photoresponse spectra taken under the same reverse bias.

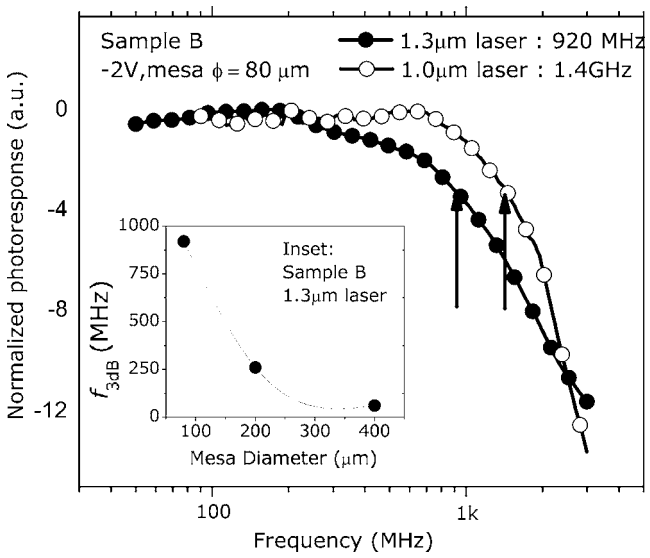

FIG. 4. Photoresponse of sample B: GaAs/GaAsSbN/GaAs photodiodes (80 μm mesa diameter) under laser excitations at 1.3 and 1.0 μm and −2 V reverse bias. Inset: Plot of 3 dB cutoff frequency vs mesa diameter. (The line serves as guide for the eyes.)

in terms of $f_{3\ \mathrm{dB}}$, it is important to mention that the device performance is *RC* time-constant limited. At −1 V bias, the capacitances of samples A and B obtained from the *C-V* measurement in Fig. 1 are ~16 and ~9 pF, respectively. The capacitance (C), resistance (R), and $f_{3\ \mathrm{dB}}$ are correlated by the following equation:

$$f_{3\ \mathrm{db}_m} = \frac{1}{2\pi RC}, \tag{5}$$

On a 50 Ω measurement system, these C values will result in $f_{3\ \mathrm{dB}}$ of 200 and 360 MHz for samples A and B, respectively. The calculated $f_{3\ \mathrm{dB}}$ values are consistent with the experimental values, where sample B has higher $f_{3\ \mathrm{dB}}$ than sample A. Subsequently, the *RC* time-constant limit can be lowered by reducing the mesa diameter of the device.

Figure 4 shows the normalized photoresponse of sample B with mesa diameter of 80 μm, under different laser excitation wavelengths of 1.0 and 1.3 μm. The plot of 3 dB cutoff frequency versus mesa diameter at 1.3 μm laser excitation is shown in the inset. It can be seen that by changing the laser excitation wavelength from 1.0 to 1.3 μm, the $f_{3\ \mathrm{dB}}$ was reduced from 1.4 GHz to 920 MHz. This difference in $f_{3\ \mathrm{dB}}$ is possibly due to the lower dc responsivity at 1.3 μm (see inset of Fig. 3), which suggests lower absorption coefficient and higher penetration length at 1.3 μm. This may have caused the photocarriers generated by 1.3 μm laser excitation to be more homogeneously distributed within the *i* layer and interact more homogeneously with material defects, resulting in the lower $f_{3\ \mathrm{dB}}$. Furthermore, it was observed that by reducing the mesa diameter by a factor of ~2, the $f_{3\ \mathrm{dB}}$ value improved by a factor of ~4. Thus the $f_{3\ \mathrm{dB}}$ is inversely proportional to the area of the mesa structure, and this further confirms the *RC* time-constant limited nature of the photodiode dynamic response.

The photoresponse and dark current characteristic of the photodiodes suggest that reducing the growth temperature of the GaAsSbN *i* layer helps us to improve its material quality. This is also supported by the asymmetrical reciprocal space map (RSM) of the XRD in [115] crystal orientation, as shown in Fig. 5. The horizontal ($q_{[1\bar{1}0]}$) and vertical ($q_{[001]}$) axes are in reciprocal lattice units (10^4 Å^{-1}), where $q_{[1\bar{1}0]}$ represents the $[1\bar{1}0]$ plane perpendicular to the substrate, and $q_{[001]}$ represents the [001] plane parallel to the substrate. All RSMs of the XRD show the GaAsSbN peak and GaAs peak located directly on one vertical line, indicating similar in-plane lattice parameter between the GaAsSbN *i* layer and GaAs substrate. The RSMs of both samples exhibit signs of atomic concentration fluctuations near the GaAs peak (marked with dashed arrows). The reduction of the diffused scattering observed in Fig. 5 suggests an improvement of GaAsSbN material quality caused by reduction of the growth temperature. This is probably due to the reduction in the point defects–induced long range atomic charge fluctuations. The DLTS study will aim to provide further insight into the type of defect states that are present in this material.

B. DLTS spectra of GaAs/GaAsSbN/GaAs photodiodes

The DLTS spectra of the majority carrier (Fig. 6) were obtained from the photodiodes using sampling number N =512, filling pulse of −0.01 V, filling pulse duration of 40 ms, and period width of 2 ms. Since sample A exhibits higher dark current than sample B, a lower reverse bias voltage was chosen for sample A (−2 V for sample A and −4 V for sample B). As seen in Table I, all four DLTS peaks exhibit broadening as indicated by the FWHM/T_p, which is the ratio between the full width at half maximum (FWHM) of the DLTS signal and its respective peak temperature (T_p). The FWHM/T_p values are all larger than the DLTS peak value from an ideal point defect, where the expected FWHM/T_p is ~0.1.[29] The broadening of the DLTS spectra suggests that the defect states may have a continuous distribution of states or discrete but closely spaced energy levels due to a distribution of isolated point defects or point defect

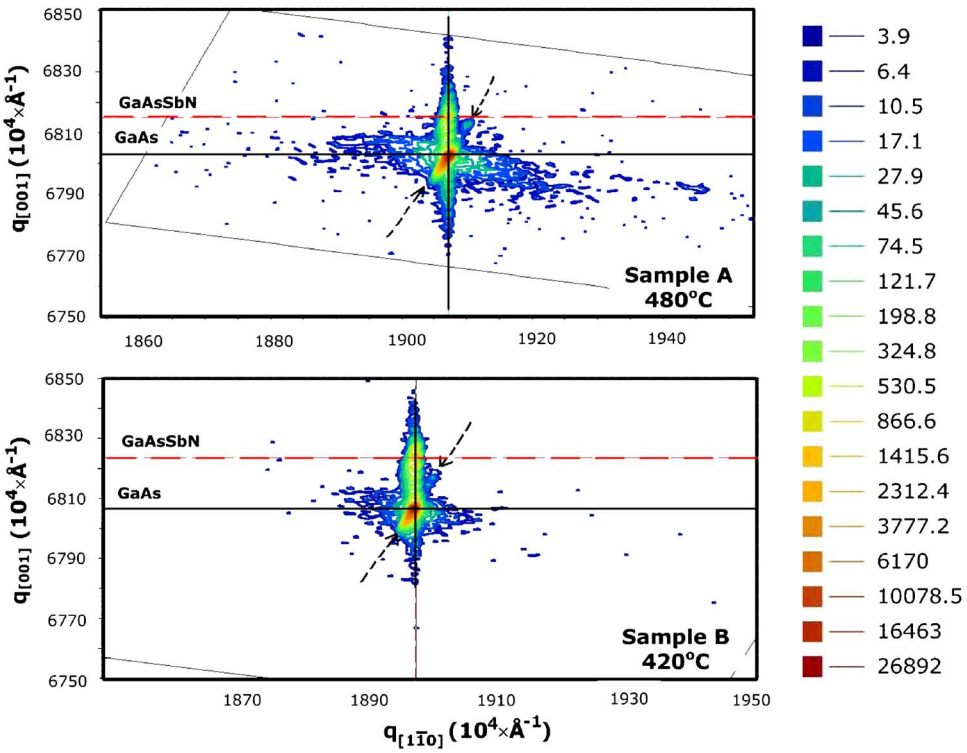

FIG. 5. (Color online) Asymmetrical reciprocal space maps of *p-i-n* samples in the [115] crystal orientation. The $K\alpha_1$ of Cu is used as the x-ray source with a wavelength of 1.540 56 Å corresponding to x-ray photon energy of 8.05 keV. The dashed arrows indicate signs of local concentration fluctuations, while the diffused scattering suggests the presence of point defects. The horizontal ($q_{[1\bar{1}0]}$) and vertical ($q_{[001]}$) axes are in reciprocal lattice units ($10^4 \times$ Å^{-1}). The GaAs (black solid line) and GaAsSbN (dashed red line) peaks are located on one vertical line, indicating closely lattice-matched condition.

clusters. However, it is important to note that this broadening does not change the peak temperature of the DLTS peak for a given rate window,[30] which allows the trap activation energy to be obtained from Eq. (3).

Each photodiode exhibits two hole traps (HT_1 and HT_2), with their respective Arrhenius plots shown in the inset of Fig. 6. Subscripts 1 and 2 indicate the first (low temperature) and the second (high temperature) defect peaks, while subscripts A and B indicate the samples from which the defect peak was originated. The spectra of HT_1 were multiplied by 10 and HT_{2B} was multiplied by 2 for clarity. By lowering the growth temperature from 480 to 420 °C, the HT_1 DLTS signal maxima increases by approximately two times and the HT_2 DLTS signal maxima decreases by ~17 times. The hole traps HT_{1A} and HT_{1B} have activation energies of 0.12 and 0.10 eV, respectively (Table I). These values are within the range for N-related shallow hole traps in GaNAs (0.03–0.18 eV above the VBM) and GaInNAs (0.10–0.21 eV above the VBM).[9,22] Thus, the HT_1 defect states are most likely to be related to the N–N and N–As defects. On the other hand, HT_{2A} and HT_{2B} trap levels have activation energies of 0.42 and 0.43 eV, respectively. The HT_2 hole traps are located close to midgap; approximately 0.46–0.47 of the *i*-layer band gap energy (E_g), which is relatively close to the $0.43E_g$ reported for EL2 defect in GaAs.[45] LT GaAs grown under similar growth temperature (~400 °C) also reported high concentrations of EL2 (~10^{19} cm^{-3}) and EL2$^+$(<5×10^{17} cm^{-3}).[19] The formation of As_{Ga} defects in GaNAs grown at low temperature under As-rich conditions has also been predicted.[8] We have observed similar As_{Ga}-related midgap defects with activation energy ~$0.43E_g$ in GaAs/GaInNAs/GaAs and GaAs/GaInNAs:Sb/GaAs photodiodes.[28] The midgap defects act as nonradiative recombination centers which effectively degrade the GaInNAs/GaAs photodiode responsivity. The reduction of the midgap trap greatly improves the responsivity of the GaInNAs:Sb/GaAs photodiode. Although Sb_{Ga} defects found on GaAs:Sb/GaAs were known to form a midgap defect state,[46] the activation energy of the midgap defect states found in this work ($0.46–0.47E_g$) is much closer to the value of the As_{Ga} defects ($0.43E_g$) than that of Sb_{Ga} defects ($0.40E_g$). Thus, it is plausible that the HT_2 defect states found in this work may have also originated from the As_{Ga} defects.

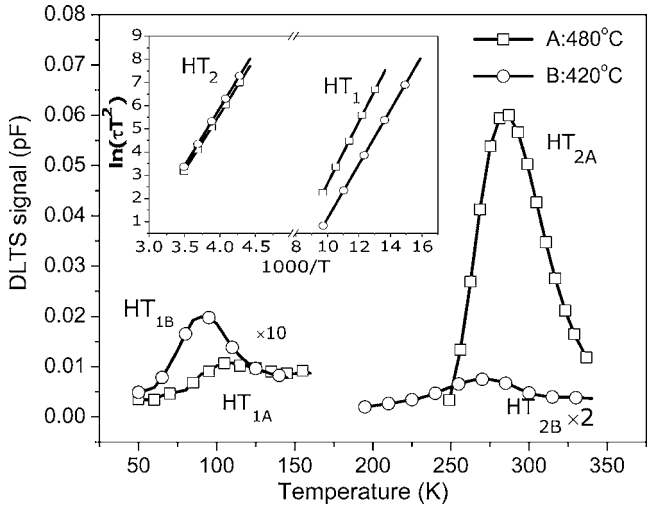

FIG. 6. DLTS spectra of photodiodes obtained using filling pulse of −0.01 V, pulse duration of 40 ms, and period width of 2 ms. Reverse bias are −2 and −4 V for samples A and B, respectively. Activation energy and hole capture cross sections were determined from the Arrhenius plots shown in the inset.

In order to examine the true activation energy of these hole traps, the hole capture cross sections were measured by

TABLE I. Trap parameters determined from DLTS analysis. FHWM/T_p is the ratio of the DLTS peaks' full width at half maxima (FWHM) and their respective peak temperature. The DLTS spectra exhibit FWHM/T_p values >0.1, suggesting a continuous distribution of states or discrete but closely spaced energy levels due to a distribution of isolated point defects or point defect clusters.

Hole trap	Sample	FWHM/T_p	Activation energy E_a (eV) (ratio with E_g)	Cross-section activation energy E_σ (eV)	Energy level (eV)	Trap concentration (cm^{-3})	Apparent carrier capture cross section σ_∞ (cm^2)
HT_{1A}	A:480 °C	0.56	0.12 (0.13E_g)	0.07	E_v+0.05	1×10^{14}	2.9×10^{-17}
HT_{1B}	B:420 °C	0.59	0.10 (0.11E_g)	0.05	E_v+0.05	7×10^{14}	2.4×10^{-17}
HT_{2A}	A:480 °C	0.17	0.42 (0.46E_g)	0.24	E_v+0.17	4×10^{15}	6.6×10^{-17}
HT_{2B}	B:420 °C	0.32	0.43 (0.47E_g)	0.26	E_v+0.18	1×10^{15}	8.2×10^{-17}

varying the filling pulse time (t_p) at the temperature where the DLTS signal maxima occurred. In the case of an ideal point defect, the capacitance transient will have an exponential shape, and the plot of $\ln(1-\Delta C_0/\Delta C_0^\infty)$ vs t_p will form a straight line with c_p as its slope. The relation between the transient amplitude ΔC_0 and t_p can be described as

$$\Delta C_0 = \Delta C_0^\infty[1-\exp(-c_p t_p)], \tag{6}$$

where ΔC_0^∞ is the saturated amplitude of the capacitance transient and c_p is the hole capture rate. However, this behavior was not observed in the plot of $\ln(1-\Delta C_0/\Delta C_0^\infty)$ vs t_p of the hole traps in Fig. 7. The DLTS signal of HT_{1A} increases monotonically following increase in the filling pulse, and the subsequent $\ln(1-\Delta C_0/\Delta C_0^\infty)$ vs t_p plot shown on the inset does not exhibit a straight line as anticipated. The behavior was observed in all of the other hole traps as well. The $\ln(1-\Delta C_0/\Delta C_0^\infty)$ vs t_p plot suggests that the hole traps behavior are more like an extended defect than an ideal point defect with a distinct energy level. In the case of an extended defect state, the hole capture rate will be a function of the logarithmic of the filling pulse,[31] and this behavior has also been reported in various DLTS studies on GaInNAs.[23,27,28] Nevertheless, Balcioglu *et al.*[23] suggested that one can still obtain the hole capture rate from the initial slope of the plot, as shown in the inset of Fig. 7, using the correlation with the hole capture cross section,

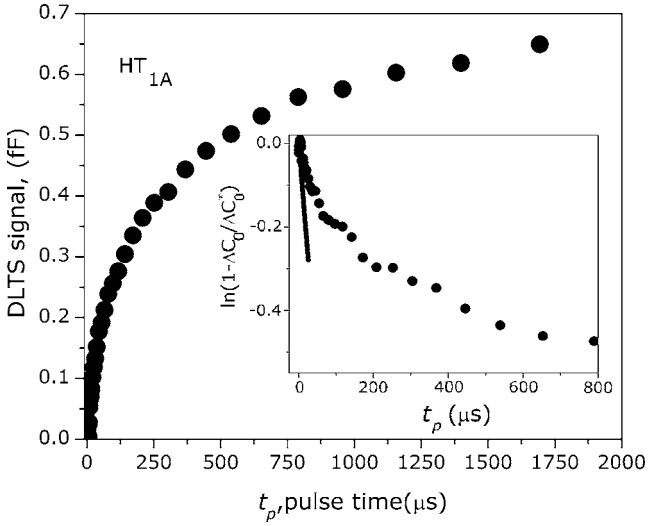

FIG. 7. Plot of DLTS signal vs filling pulse (t_p) for HT_{1A}. The plot $\ln(1-\Delta C_0/\Delta C_0^\infty)$ as function of t_p is shown in the inset, where the capture rate was determined from the initial slope.

$$c_p = \sigma_p \langle v_{\text{th}} \rangle p, \tag{7}$$

where v_{th} is the thermal velocity and p is the hole concentration. Thus, using Eq. (7), the cross-section activation energy of HT_{1A} was determined to be 0.07 eV, suggesting that its energy level is 0.05 eV above the VBM. The cross-section activation energies and the trap energy levels of HT_{1A}, HT_{1B}, Ht_{2A}, and HT_{2B} are listed in Table I.

Reduction in the *i*-layer growth temperature from 480 to 420 °C has two implications on the deep level spectra: (i) the concentration of shallow N-related traps (HT_1) increases (from 1×10^{14} to 7×10^{14} cm^{-3}) and (ii) the concentration of midgap traps (HT_2) decreases (from 4×10^{15} to 1×10^{15} cm^{-3}). At first glance, this trend defies the general principle that the trap concentrations of HT_2 increase and HT_1 reduces as the growth conditions become more As rich (i.e., increased V/III ratio, reduced growth temperature). However, similar to As_{Ga} defects, the formation energy of $As_{Ga}-N_{As}$ defects also decreases following reduction in the growth temperature. This is significant, because the formation of $As_{Ga}-N_{As}$ pairs will push the As_{Ga} midgap state nearer to the VBM.[8] This explains the decrease in the midgap trap concentration in sample B and the increase in shallow N-related trap concentration as the growth temperature is lowered and the growth condition moves toward the As-rich condition. Since the midgap trap level acts as nonradiative recombination centers in GaAs and GaInNAs, the decrease in the midgap trap level in sample B also explains the improvement in the photoresponse observed in Fig. 3. The overall reduction in trap concentration in sample B also correlates with the reduction in the diffused scattering of the XRD RSM, as shown in Fig. 5. However, the information revealed by DLTS can only offer a broad picture of the defect states in GaAsSbN. A more precise study involving first-principles simulation within the density functional theory (DFT) is required to confirm the stability of the aforementioned defects and their position in reference to the band gap of GaAsSbN. Experiment techniques such as optically detected electron paramagnetic resonance[19,46,47] and x-ray absorption spectroscopy[7,48,49] are essential tools to study the atomic and electronic structures of the defects. These theoretical and experimental experiments on GaAsSbN are currently still lacking.

IV. CONCLUSION

DLTS measurements on GaAs/GaAsSbN/GaAs reveal two types of defect states in the GaAsSbN *i* layer: (i) HT_1: a

shallow N-related trap ($E_a \sim 0.10-0.12$ eV) and (ii) HT_2: midgap trap with $E_a \sim 0.42-0.43$ eV. Reduction in growth temperature from 480 to 420 °C reduces the HT_2 trap concentration from 4×10^{15} to 1×10^{15} cm^{-3}, while increases the HT_1 trap concentration from 1×10^{14} to 7×10^{14} cm^{-3}. Reduction in the HT_2 trap concentration following growth temperature reduction was attributed to the reduction of As_{Ga} point defect-related midgap defects, as also suggested by comparison of the XRD reciprocal space maps. Evidence of possible change from the As_{Ga}-related midgap state to a shallow level defect due to the formation of $As_{Ga}-N_{As}$ pairs was suggested by the increase of the HT_1 trap concentration. An ~4 dBm improvement in photoresponse under 1.3 μm laser excitation and approximately eight times reduction in dark current at −8 V reverse bias were attributed to the reduction in the overall trap concentration and mainly the As_{Ga} midgap trap concentration in the sample grown at 420 °C.

ACKNOWLEDGMENTS

This work was partly supported by the European Commission within the European Network of Excellence ISIS, www.ist-isis.org, under Grant No. 26592. Also, the support from THALES@NTU laboratory and MERLION Program from the French Embassy in Singapore are gratefully acknowledged.

[1] G. Ungaro, G. Le Roux, R. Teissier, and J. C. Harmand, Electron. Lett. **35**, 1246 (1999).
[2] H. B. Yuen, S. R. Bank, M. A. Wistey, J. S. Harris, S. Maeng-Je, Y. Seokhyun, R. Kudrawiec, and J. Misiewicz, J. Appl. Phys. **97**, 113510 (2005).
[3] H. B. Yuen, S. R. Bank, M. A. Wistey, J. S. Harris, and A. Moto, J. Appl. Phys. **96**, 6375 (2004).
[4] H. Luo, J. A. Gupta, and H. C. Liu, Appl. Phys. Lett. **86**, 211121 (2005).
[5] S. Wicaksono, S. F. Yoon, K. H. Tan, and W. K. Loke, J. Vac. Sci. Technol. B **23**, 1054 (2005).
[6] S. Wicaksono, S. F. Yoon, W. K. Loke, K. H. Tan, and B. K. Ng, J. Appl. Phys. **99**, 104502 (2006).
[7] G. Ciatto, J. C. Harmand, L. Largeau, and F. Glas, Phys. Status Solidi **3**, 1931 (2006).
[8] S. B. Zhang and S.-H. Wei, Phys. Rev. Lett. **86**, 1789 (2001).
[9] A. Janotti, S.-H. Wei, S. B. Zhang, S. Kurtz, and C. G. Van de Walle, Phys. Rev. B **67**, 161201 (2003).
[10] L. Wei, M. Pessa, and J. Likonen, Appl. Phys. Lett. **78**, 2864 (2001).
[11] W. J. Fan, S. F. Yoon, T. K. Ng, S. Z. Wang, W. K. Loke, R. Liu, and A. Wee, Appl. Phys. Lett. **80**, 4136 (2002).
[12] S. G. Spruytte, C. W. Coldren, J. S. Harris, W. Wampler, P. Krispin, K. Ploog, and M. C. Larson, J. Appl. Phys. **89**, 4401 (2001).
[13] T. Ahlgren, E. Vainonen-Ahlgren, J. Likonen, W. Li, and M. Pessa, Appl. Phys. Lett. **80**, 2314 (2002).
[14] L. Wei, M. Pessa, T. Ahlgren, and J. Decker, Appl. Phys. Lett. **79**, 1094 (2001).
[15] N. Q. Thinh, I. A. Buyanova, P. N. Hai, W. M. Chen, H. P. Xin, and C. W. Tu, Phys. Rev. B **63**, 033203 (2001).
[16] N. Q. Thinh, I. A. Buyanova, W. M. Chen, H. P. Xin, and C. W. Tu, Appl. Phys. Lett. **79**, 3089 (2001).
[17] J. I. Landman, C. G. Morgan, and J. T. Schick, Phys. Rev. Lett. **74**, 4007 (1995).
[18] M. A. Pinault and E. Tournie, Appl. Phys. Lett. **79**, 3404 (2001).
[19] K. Krambrock, M. Linde, J. M. Spaeth, D. C. Look, D. Bliss, and W. Walukiewicz, Semicond. Sci. Technol. **7**, 1037 (1992).
[20] J. Alam *et al.*, Philos. Mag. **86**, 3477 (2006).
[21] F. Abulfotuh, A. Balcioglu, D. Friedman, J. Geisz, and S. Kurtz, AIP Conf. Proc. **462**, 492 (1999).
[22] D. Kwon, R. J. Kaplar, S. A. Ringel, A. A. Allerman, S. R. Kurtz, and E. D. Jones, Appl. Phys. Lett. **74**, 2830 (1999).
[23] A. Balcioglu, R. K. Ahrenkiel, and D. J. Friedman, Appl. Phys. Lett. **76**, 2397 (2000).
[24] R. J. Kaplar, D. Kwon, S. A. Ringel, A. A. Allerman, S. R. Kurtz, E. D. Jones, and R. M. Sieg, Sol. Energy Mater. Sol. Cells **69**, 85 (2001).
[25] R. J. Kaplar, S. A. Ringel, S. R. Kurtz, J. F. Klem, and A. A. Allerman, Appl. Phys. Lett. **80**, 4777 (2002).
[26] A. J. Ptak, S. W. Johnston, S. Kurtz, D. J. Friedman, and W. K. Metzger, J. Cryst. Growth **251**, 392 (2003).
[27] S. Y. Xie, S. F. Yoon, and S. Z. Wang, J. Appl. Phys. **97**, 073702 (2005).
[28] W. K. Loke, S. F. Yoon, K. H. Tan, S. Wicaksono, and W. J. Fan, J. Appl. Phys. **101**, 033122 (2007).
[29] L. C. Kimerling and J. R. Patel, Appl. Phys. Lett. **34**, 73 (1979).
[30] P. Omling, L. Samuelson, and H. G. Grimmeiss, J. Appl. Phys. **54**, 5117 (1983).
[31] T. Wosinski, J. Appl. Phys. **65**, 1566 (1989).
[32] S. Weiss and R. Kassing, Solid-State Electron. **31**, 1733 (1988).
[33] D. V. Lang, J. Appl. Phys. **45**, 3023 (1974).
[34] J. E. Cunningham *et al.*, J. Vac. Sci. Technol. B **19**, 1948 (2001).
[35] P. Delvin, H. M. Heravi, and J. C. Woolley, Can. J. Phys. **52**, 743 (1981).
[36] W. Shan, W. Walukiewicz, J. W. Ager, E. E. Haller, J. F. Geisz, D. J. Friedman, J. M. Olson, and S. R. Kurtz, Phys. Rev. Lett. **82**, 1221 (1999).
[37] F. Bousbih, S. B. Bouzid, R. Chtourou, F. F. Charfi, J. C. Harmand, and G. Ungaro, Mater. Sci. Eng., C **21**, 251 (2002).
[38] Y. X. Dang, W. J. Fan, S. T. Ng, S. Wicaksono, S. F. Yoon, and D. H. Zhang, J. Appl. Phys. **98**, 026102 (2005).
[39] J. C. Harmand *et al.*, Semicond. Sci. Technol. **17**, 778 (2002).
[40] P. R. C. Kent and A. Zunger, Phys. Rev. Lett. **86**, 2613 (2001).
[41] I. Vurgaftman, J. R. Meyer, and L. R. Ram-Mohan, J. Appl. Phys. **89**, 5815 (2001).
[42] S.-H. Park, J. Appl. Phys. **100**, 043113 (2006).
[43] Y. Zhang, A. Mascarenhas, H. P. Xin, and C. W. Tu, Phys. Rev. B **61**, 4433 (2000).
[44] E. Arola, J. Ojanen, H.-P. Komsa, and T. T. Rantala, Phys. Rev. B **72**, 045222 (2005).
[45] F. D. Auret, A. W. R. Leitch, and J. S. Vermaak, J. Appl. Phys. **59**, 158 (1986).
[46] P. Omling, B. H. Yang, L. Samuelson, R. Yakimova, J. O. Fornell, and L. Ledebo, Phys. Rev. B **44**, 13398 (1991).
[47] M. Baeumler, J. Schneider, U. Kaufmann, W. C. Mitchel, and P. W. Yu, Phys. Rev. B **39**, 6253 (1989).
[48] G. Ciatto *et al.*, Phys. Rev. B **68**, 161201 (2003).
[49] G. E. Ice, C. J. Sparks, A. Habenschuss, and L. B. Shaffer, Phys. Rev. Lett. **68**, 863 (1992).